ACS Editors' Choice

Environmental Science & Technology

Article

pubs.acs.org/est

Terms of Use

Assessment of Dry and Wet Atmospheric Deposits of Radioactive Aerosols: Application to Fukushima Radiocaesium Fallout

Marc-André Gonze,*[,†] Philippe Renaud,[†] Irène Korsakissok,[‡] Hiroaki Kato,[§] Thomas G. Hinton,[†] Christophe Mourlon,[†] and Marie Simon-Cornu[†]

[†]Institute for Radiological Protection and Nuclear Safety (IRSN), Environmental Research Division, BP 3−13115 St-Paul-lez-Durance Cedex, France

[‡]Institute for Radiological Protection and Nuclear Safety (IRSN), Nuclear & Radiological Emergency Division, BP 17−92262 Fontenay-aux-Roses Cedex, France

[§]Center for Research in Isotopes and Environmental Dynamics, University of Tsukuba,1-1-1 Tennodai, Tsukuba, Ibaraki Japan

Supporting Information

ABSTRACT: The Fukushima Dai-ichi nuclear accident led to massive atmospheric deposition of radioactive substances onto the land surfaces. The spatial distribution of deposits has been estimated by Japanese authorities for gamma-emitting radionuclides through either airborne monitoring surveys (since April 2011) or in situ gamma-ray spectrometry of bare soil areas (since summer 2011). We demonstrate that significant differences exist between the two surveys for radiocaesium isotopes and that these differences can be related to dry deposits through the use of physically based relationships involving aerosol deposition velocities. The methodology, which has been applied to cesium-134 and cesium-137 deposits within 80-km of the nuclear site, provides reasonable spatial estimations of dry and wet deposits that are discussed and compared to atmospheric numerical simulations from the Japanese Atomic Energy Agency and the French Institute of Radioprotection and Nuclear Safety. As a complementary approach to numerical simulations, this field-based analysis has the possibility to contribute information that can be applied to the understanding and assessment of dose impacts to human populations and the environment around Fukushima.

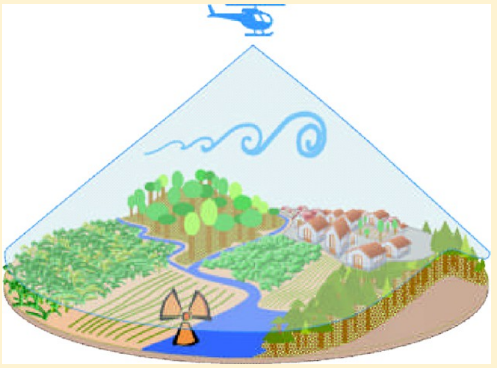

INTRODUCTION

The accident that damaged the Fukushima Daiichi Nuclear Power Plant (FDNPP) site in March 2011 resulted in massive atmospheric releases of radioactive substances (mainly iodine, cesium and tellurium isotopes) that were dispersed and deposited onto the continental and oceanic surfaces. The widespread deposition resulted in populations being exposed to γ radiation from external exposure or through the ingestion of contaminated foodstuffs. The most seriously contaminated terrestrial areas are within 80km of the damaged site, and comprise forests (70%), agricultural fields or meadows (20%), and inhabited areas (10%). The characteristics of these releases and the conditions under which they dispersed have been assessed in detail, through numerical studies in combination with activity and ambient dose rate measurements obtained during the accident phase.[1−10] However, the duration and complexity of this accident were such that there are still gaps in our knowledge. These mainly concern the exact sequence of releases, their isotopic composition, plume dispersion in coastal and mountainous areas, and the characteristics of the atmospheric deposition events.

Knowledge of the relative contributions of dry and wet deposition is an important element of the postaccident analysis because it determines the initial interception and retention of airborne radioactive particles by plant canopies, their subsequent transfer pathways in soil-plant systems and their dose impact to humans. Dry deposition onto vegetation of especially fine aerosols (i.e., smaller than a few microns in diameter, typically) is known to increase with the aerial biomass of vegetation, or leaf area index, due to both an increase in the interception surface and atmospheric turbulence.[11−17] For fallout induced by precipitation, the interception fraction (i.e., proportion of the deposit which is intercepted by the above ground biomass) also increases with biomass but strongly decreases with rainfall, at least for moderate to intense events, due to water and particle dripping.[18−22] This interception fraction strongly influences the fate of deposited radionuclides in the terrestrial systems, as part of the radioactivity initially retained by vegetation is progressively incorporated in the living biomass, then exported and harvested in case of cropping systems. For forest ecosystems, knowledge of interception

Received: June 2, 2014
Revised: September 3, 2014
Accepted: September 5, 2014
Published: September 5, 2014

fraction is equally important as it controls contaminant fluxes to soil or biota, as well as ambient gamma-ray radiations within the forest.

The aim of this paper is to specify and test a complementary approach to atmospheric numerical simulations for rapidly estimating the spatial distribution of dry and wet deposits of gamma-ray emitting radionuclides following an accident. The method is based on the analysis of two kinds of measurements of the radioactive deposits in the areas impacted by the accident: (1) measurements by *in situ* spectrometry of bare soils in inhabited areas, and (2) measurements by airborne gamma-ray spectrometry which integrates radiation from the underlying land surfaces. The key idea is to attribute differences in deposition, as measured by the two field techniques, to mainly the signature of dry deposition, because dry deposition is much more sensitive to the characteristics of the land surface than wet deposition. The approach, its underlying assumptions and limitations are first discussed, then applied to cesium-134 (half-life: 754 days) and cesium-137 (half-life: 10972 days) within 80 km of the FDNPP site. The spatial estimation of dry and wet contributions to the total deposits are then discussed and compared to predictions by atmospheric numerical studies performed by the Japanese Atomic Energy Agency (JAEA) and the French Institute of Radioprotection and Nuclear Safety (IRSN).

MATERIALS

This study is based on two different and totally independent monitoring surveys of radiocaesium deposits in the contaminated region of Fukushima (both being expressed in Becquerels per unit surface area, i.e. Bq m^{-2}), estimated from either in situ spectrometry of bare soils in inhabited areas or airborne gamma-ray monitoring of the land surface. Both data sets were published and made available on the Internet (see hereafter for references).

Bare Soil Survey. In summer 2011, the Japan Atomic Energy Agency (JAEA) coordinated an extensive field survey of radioactive contamination in soils in the eastern part of Fukushima Prefecture, with a focus on the 9000 km^2 area, within an 80 km radius of the FDNPP.[23,24] About 2200 sampling stations were established on a regular grid with an approximately 2 × 2 km^2 square mesh. These stations were located mainly in undisturbed soil areas of inhabited environments, such as gardens, school yards or other bare soil surfaces. For those areas which were occupied by sparse natural vegetation, like weeds and other herbaceous species, plants were included in the samples. The inventories of gamma-emitters such as ^{134}Cs and ^{137}Cs were estimated in the top 5 cm soil layer, from five soil samples collected within a 3 × 3 m^2 area at each station. This sampling was accompanied by a gamma-ray measurement taken at 1 m height above soil, right in the middle of the square. The soil deposit and dose rate values were reported as of June 14, 2011, by applying a physical decay correction factor specific to each isotope.

Land Surface Survey. Airborne gamma-ray monitoring surveys have been regularly carried out since April 2011 in Fukushima Prefecture and the neighboring Prefectures.[25] They were operated by the Japanese Ministry of Education, Culture, Sports, Science and Technology (MEXT), in collaboration with the U.S. Department of Energy, the JAEA and Japanese Prefectures. Gamma measurements were conducted from airplane/helicopter flying at altitudes which varied from 150 to 300 m above ground, along routes separated from each other by about 1.8 km. As stated in the survey reports, the flux of photons measured by the NaI instrument within the aircraft included contributions of primary and scattered photons emitted from a mixture of contaminated objects below the aircraft, in a roughly 90° cone of view (see Figure 1). These objects consisted of soils, vegetation, water surfaces, and various anthropogenic items such as roads and buildings.

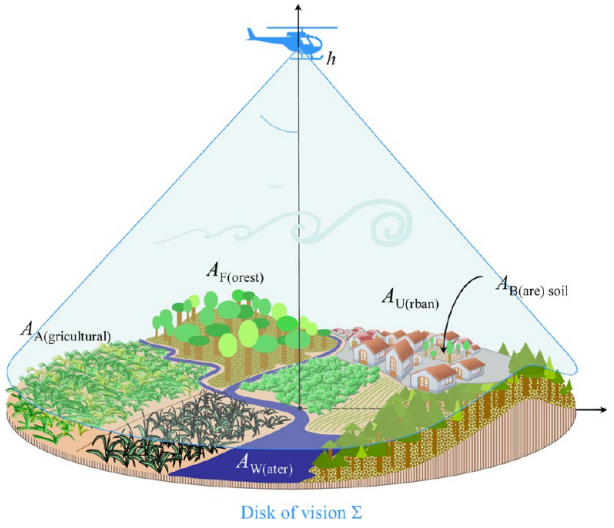

Figure 1. Schematical representation of the field of view of an airborne detector flying at altitude *h* above soil and consisting of a mixture of spatially distributed aquatic and terrestrial surfaces.

Thus, for a detector located at flying altitude *h*, the "visible" land surface can be defined approximately by a circle of roughly *h* radius. This "visible" disk is denoted as "Σ" hereafter. The method for transforming count rates at flying altitude to radioactive deposit at ground level required three conversion factors: (1) an altitude correction function for extrapolating count rates to 1-m height above ground; (2) a dose-rate conversion coefficient for converting then count rates into dose rates and (3) a coefficient for converting dose rates into ground deposit. Relatively accurate conversion coefficients were first estimated from validation surveys established on the ground in late 2011, in the so-called "fourth airborne survey". The coefficients were obtained by measuring count rates at varying flight altitudes and then obtaining the corresponding in situ dose rates at 1 m height. The actual readings of the fourth campaign were converted as of November 5, by applying a physical decay correction factor, and discretized into classes of values, ranging from <10 to >3000 kBq m^{-2}.

METHODS

Method Overview. The approach for assessing the spatial distribution of dry and wet fractions relies on the idea that spatial differences in deposition observed by the two different field techniques (after relevant space and time preprocessing) are likely caused by dry deposition processes. Unlike wet deposition, dry deposition of airborne particles strongly depends on the characteristics of the surface on which they deposit, because most of the underlying mechanisms are known to be enhanced by the surface roughness, as is evident in well-developed collecting surfaces such as vegetation canopies. This dependence upon the surface characteristics is especially important for fine particles, smaller than a few micrometers,

as gravitational settling becomes negligible with regards to other mechanisms. Consequently, in all locations where dry deposition contributes in a significant way, the land surface deposit over Σ (denoted A_Σ) may noticeably differ from bare soil deposits averaged over Σ (denoted A_B). As depicted in Figure 1, the different objects within Σ regions can be classified into four "land use categories", each dominated by forests, agricultural fields, aquatic surfaces or urban environments. The latter includes the investigated bare soil areas. Deposition in each land use category i (denoted A_i) and bare soil areas (A_B) results from both dry and wet contributions. If it is assumed that, first, dry deposition can be estimated from radioactivity concentration in air through the use of a characteristic deposition velocity specific to each i and second, wet deposition is uncorrelated to landuse occupancy at infra-kilometer scales (i.e., within Σ), then the method has the possibility to reasonably estimate dry and wet contributions from the spatial comparison between A_B and A_Σ.

Data Preprocessing. To quantify spatial differences in deposition it is necessary to convert both data sets to the same reference date (set arbitrarily to March 15, 2011, here) and project them onto the same spatial frame.

Time extrapolation from March to the beginning of November 2011 (date of the fourth airborne survey) through physical decay only is justified as long as no processes other than radioactive decay were shown to play a significant role in the evolution of radiocaesium deposits. As discussed in section 1 of the Supporting Information (SI), the analysis of time series of radioactivity concentrations measured in bare soil areas of the Fukushima region strongly supports this assumption. As also discussed in section 3 of the SI, this hypothesis is likely to be valid everywhere except in nonstagnant aquatic systems where water renewal induced a rapid decrease of initial contamination, and maybe, in urban environments that have been decontaminated, either deliberately or through natural wash-off by heavy rainfalls and typhoons during summer 2011. Although time extrapolation through physical decay remains questionable for aquatic and urban environments, this method has been used for all land categories.

The spatial entities chosen for comparison purpose were Σ disks with a constant radius, on a regular grid of 0.3 × 0.3 km^2 mesh size. Two different radii were considered, 150 and 300 m, to mimic the lowest and highest altitudes reported to have been flown. Soil data have been projected onto this spatial frame by performing a spatial interpolation (i.e., kriging) on a regular grid with a 30 × 30 m^2 mesh size and averaging the interpolated field in each Σ disk. Compared to deterministic techniques, kriging has the advantage to better account for the spatial correlation between field observations at the resolved scales (i.e., greater than 2 km, here). Correlation at smaller scales could not be inferred from these field data but could be estimated at scales ranging from meters to a few tens of meters from an analysis of the contamination data set presented in section 1 of the SI. The assumptions made in the geostatistical treatment and validation tests are further discussed in section 2 of the SI.

Mathematical Formulation of Wet and Dry Deposits. The difference between bare soil (B) and land surface (Σ) deposits has been computed through the following regionalized indicator:

$$\beta = 1 - \frac{A_B}{A_\Sigma} \tag{1}$$

where A_B and A_Σ are the spatially averaged deposits over Σ (in Bq m^{-2}), at the same reference date and on the same reference spatial frame. This indicator has been computed for the two radii considered. High positive values are expected in all locations where $A_\Sigma > A_B$. Negative values are expected in three cases. Negative values can be produced in areas occupied by smooth surfaces with a characteristic deposition velocity much smaller than the bare-soil one. Values can also be negative in areas where A_Σ has decreased much faster than expected from physical decay alone, down to lower values than A_B at time of airborne survey (i.e., November 5, 2011). Such situations can be typically found in nonstagnant aquatic regions (e.g., river, lake, seaside band), or urban areas, due to short-term decontamination processes. Finally, unrealistic negative β values can result from inaccuracies in the estimated deposits, especially in regions where both quantities are expected to be similar (e.g., agricultural areas without any vegetation, areas largely dominated by wet deposition).

From eq 2 to 5, expressions for dry and wet deposits are developed and given in eqs 6a−6b. The land surface deposit can be estimated as a weighted average of the spatially averaged deposits A_i in landscape category i (in Bq m^{-2}):

$$A_\Sigma = \sum_i \alpha_i A_i \tag{2}$$

Where weighting factors α_i represent the percentage of the Σ disk area covered by i (*i.e.* $\Sigma_i \alpha_i = 1$). The α_i's depend on both geographical location and Σ radius. For each category i, the mean deposit results from dry and wet contributions:

$$A_i = A_i^{dry} + A^{wet} \tag{3}$$

Where dry deposit depends on i and wet deposit is assumed to be constant among landuse categories. As discussed in the section 3 of the SI, dry deposit can be reasonably estimated through the use of a characteristic deposition velocity, Vd_i (in m·s^{-1}), as follows:

$$A_i^{dry} = Vd_i \times C_a \tag{4}$$

Where C_a is the concentration in air at a reference height above soil (Bq m^{-3}), averaged over Σ and averaged with time over the (dry) deposition periods. In the case where A_i^{dry} results from multiple events with contrasted characteristic deposition velocities, it can be demonstrated that Vd_i can be expressed as a weighted average of event-based values (see section 3 of the SI for a mathematical expression of weighting factors). Equations 3 and 4 also hold for A_B. Combining eqs 2, 3 and 4 leads to the following expression for the bulk deposit:

$$A_\Sigma = Vd_\Sigma \times C_a + A^{wet} \tag{5}$$

Where $Vd_\Sigma = \Sigma_i \alpha_i Vd_i$ is a bulk velocity which depends on both geographical location and Σ radius. Finally, combining eq 5 with eq 3 written for bare soil and introducing β allows expressing wet and dry deposits:

$$A^{wet} = A_\Sigma \times \left(1 - \beta \times \frac{Vd_\Sigma^*}{Vd_\Sigma^* - 1}\right) \tag{6a}$$

$$A_\Sigma^{dry} = A_\Sigma \times \beta \times \frac{Vd_\Sigma^*}{Vd_\Sigma^* - 1} \tag{6b}$$

Where $Vd_\Sigma^* = \Sigma_i \alpha_i Vd_i^*$ and $Vd_i^* = Vd_i/V_B$ are normalized by the velocity onto bare soil. These equations show that in all

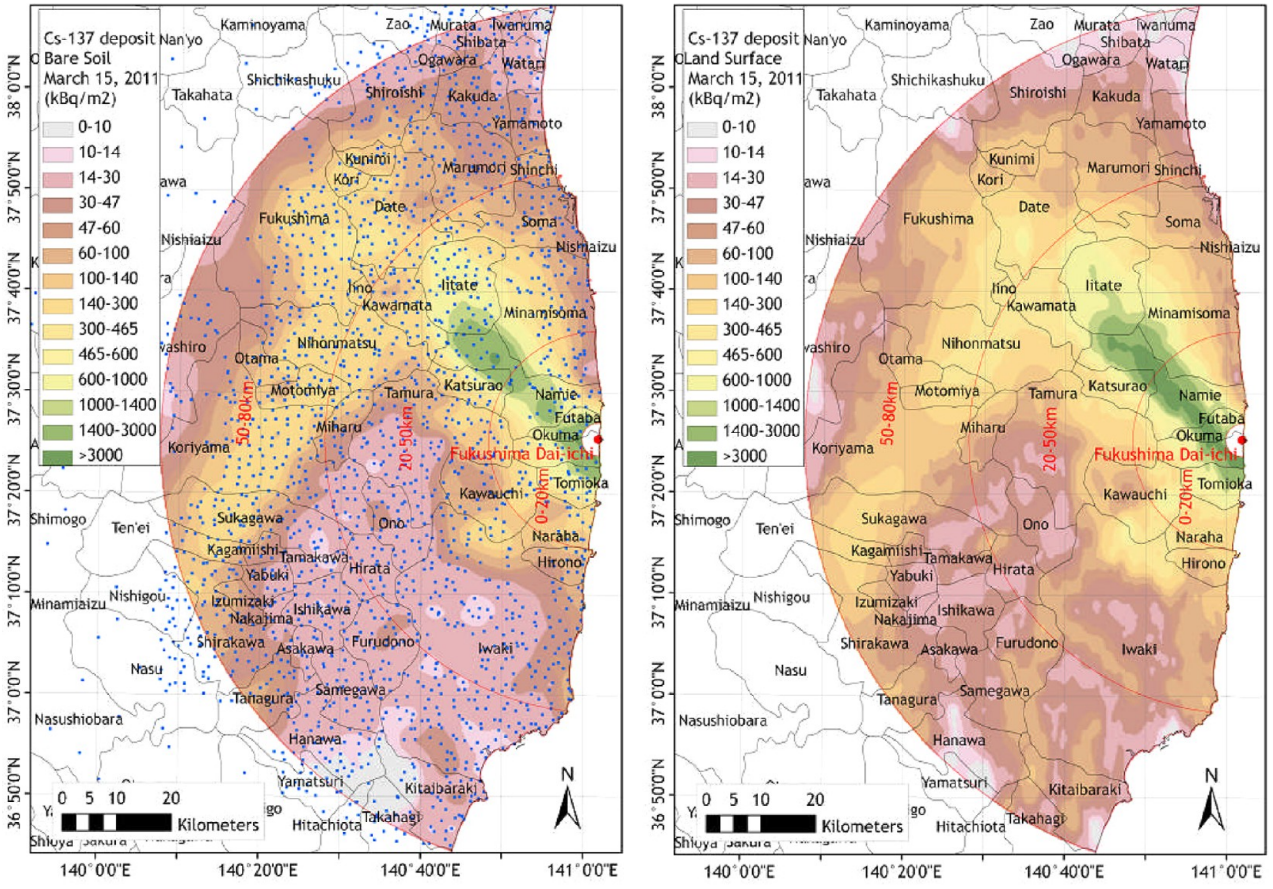

Figure 2. Spatial distribution of ^{137}Cs deposits (kBq m^{-2}) in the 80 km region of FDNPP: (a) estimated through kriging of contamination data in bare soil stations of inhabited areas (blue dots), (b) estimated at ground surface by airborne gamma-ray monitoring. Values have been converted to March 15, 2011, through decay correction.

regions where $Vd_\Sigma^* > 1$, dry contribution increases with increasing positive β's or decreasing Vd_Σ^*'s. It can also be noticed that, in regions where dry deposition greatly dominates, expected β's approach a theoretical limit $1-1/Vd_\Sigma^*$ which cannot be exceeded because $A_\Sigma^{dry} \leq A_\Sigma$ must be ensured. To avoid unphysical results, $\beta = 1-1/Vd_\Sigma^*$ was imposed when necessary. It is worth noting that eqs 6 also provide unrealistic predictions in regions where $\beta < 0$ and $Vd_\Sigma^* > 1$, as they predict $A_\Sigma^{dry} \leq 0$.

Characteristic Deposition Velocities. Applying previous equations requires providing characteristic values for Vd_i^* velocities, from which Vd_Σ^* can be computed based on a detailed land-use map. This map has been established through the processing of a Spot satellite image at spatial scales smaller than Σ diameter (i.e., a 30 m pixel resolution). Plausible ranges of variation for deposition velocity ratios onto water surfaces (Vd_W^*), agricultural surfaces (Vd_A^*), urban areas (Vd_U^*) and forests (Vd_F^*) are discussed in section 5 of the SI. Based on the assumption that the mean aerodynamic diameter of cesium particles was in the range 0.5−2 μm, Vd_A^* was shown to approximately vary between 2 (short grass) and 4 (growing crops) and Vd_F^* ranged between 5 (mixed forest) and 15 (evergreen needleleaf forest). Deposition velocity onto water surfaces was considered equal to zero in order to implicitly account for the fast decrease of deposited activity by water renewal (contribution of bed and bank sediments to the airborne γ radiation is neglected). Due to the lack of specific data for inhabited environments of Fukushima region, it was proposed to adopt the same range of variation as for agricultural environments, although this range might actually overestimate the actual bulk velocity in some urban areas (see section 5 of the SI for further discussion).

Based on these choices, Vd_Σ^* was computed for the two radii considered (i.e., 150 and 300 m) and two contrasted velocity data sets: (Vd_W^*, Vd_A^*, Vd_U^*, Vd_F^*) = (0, 2, 2, 5) or (0, 4, 4, 15). This gave 2 × 2 assessments.

Uncertainties and Limitations. For enabling the evaluation of the results achieved in the next section, it is worth considering simplifications, uncertainties and limitations in the method. Equation 6b shows that uncertainties in the spatial estimation of dry deposition ratio, $DR = A_\Sigma^{dry}/A_\Sigma$ (dimensionless), may originate from uncertainties in Vd_Σ^* and β estimates, that is A_B and A_Σ. Confidence in A_B and A_Σ at spatial scales smaller than a few kilometers may not be satisfactory because monitoring data do not permit to properly capture their spatial variability. At larger scales, confidence in A_B is rather high because sampling stations were numerous and kriging validation tests proved to be rather satisfactory (see section 2 of the SI). Confidence in A_Σ is more questionable due to time extrapolation assumption in aquatic and urban environments. Uncertainties in raw airborne data, due to the use of cps-to-Becquerels conversion coefficients, also cannot be excluded

dx.doi.org/10.1021/es502590s | Environ. Sci. Technol. 2014, 48, 11268−11276

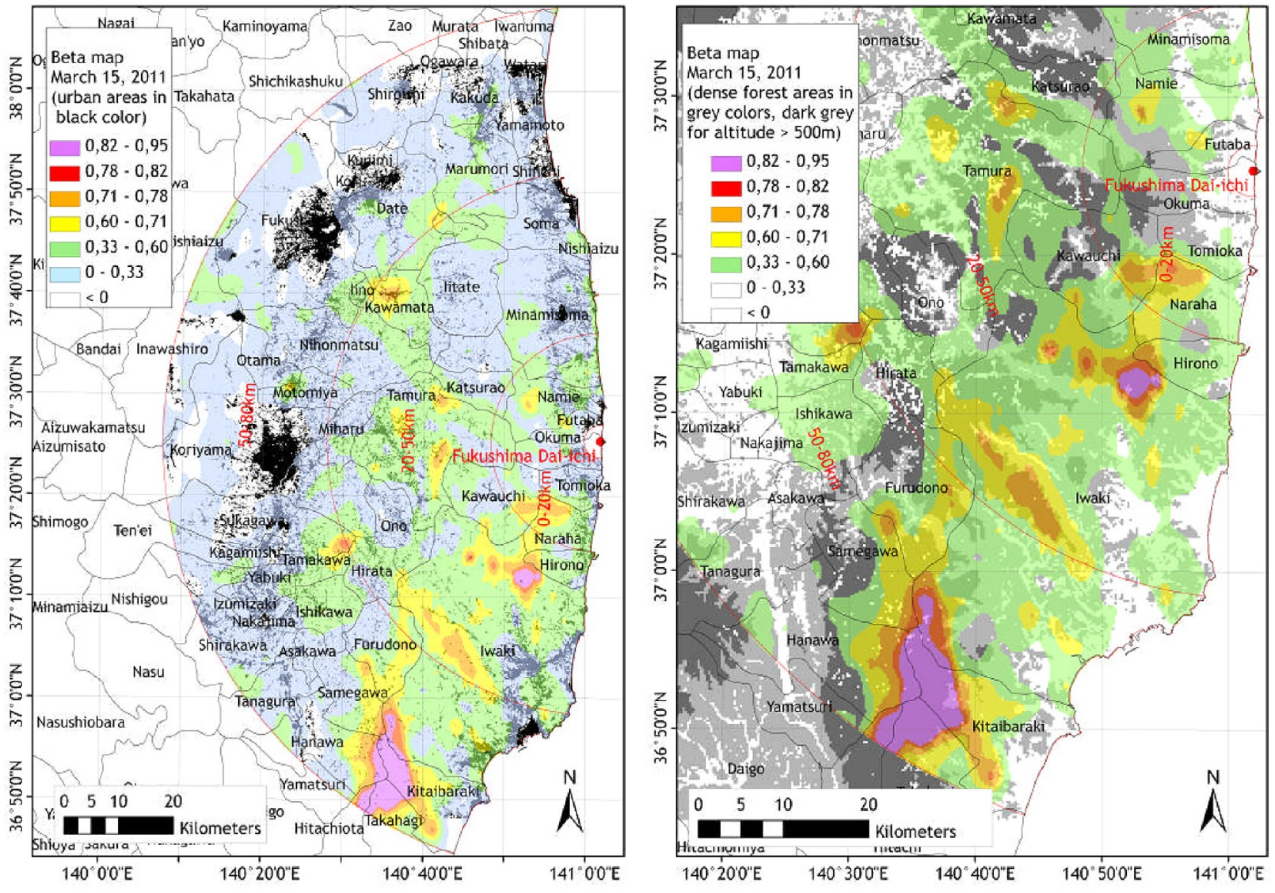

Figure 3. Spatial estimation of β indicator for ^{137}Cs in the 80-km region from FDNPP, for a 300 m averaging radius. Soil occupancy is displayed in the background: (a) urban areas in black color, (b) densely forested areas in light/dark gray color, for two different elevation ranges (light gray: 0−500m, dark gray: 500−1200m).

(but unfortunately not quantified in MEXT reports). Variability of Vd_Σ* is explicitly accounted for in this study as sensitivity to flying altitude and velocities ratios, Vd_i*, is to be evaluated through the use of two contrasted flying altitudes and deposition velocity data sets. Equation 6b shows that underestimating Vd_i* values (i.e., or underestimating Vd_Σ*) results in overestimating DR, and vice versa. Absolute error ΔDR (dimensionless) can be expressed as a weighted sum of relative errors in A_B, A_Σ, and Vd_Σ*, in which both contributions of deposits are shown to vanish for $\beta = 1$, contribution of bulk velocity vanishes for $\beta = 0$ and all contributions are shown to decrease with increasing Vd_Σ*'s values (especially for bulk velocity). Thus, if we neglect uncertainties in raw airborne data, the method is likely to produce reasonable results at large spatial scales (say greater than 10 km) in all regions apart from aquatic zones and dense urban environments. Relatively accurate results are expected in forested regions with high Vd_Σ* values (with predominant evergreen species) and high β values (say greater than 0.5).

RESULTS AND DISCUSSION

Bare Soil versus Land Surface Deposits. A_B and A_Σ are displayed in Figure 2a,b for ^{137}Cs. Although not displayed, results for ^{134}Cs were almost identical (*i.e.* isotopic ratio equal to one). Differences between maps are mainly perceptible in regions located to the south and southwest of the FDNPP site (e.g., Iwaki and neighboring towns to the west), where activities can there be 3−4 times greater than the ones estimated on bare soil surfaces. Although less pronounced, differences can also be observed to the northwest of the nuclear site in the highest contaminated areas (e.g., Namie town). In the later region, however, differences might result from kriging inaccuracies in the predicted values of A_B as exhibited by cross-validation tests (see section 2 of the SI).

The computed β is displayed in Figures 3a,b for a 300 m radius. No significant differences could be observed when averaging with a 150 m radius because the kriged field does not feature small spatial scales. Low positive values ($\beta < 0.33$) were basically observed in the dense agricultural areas of Abukuma valley and the high-elevation forested volcano areas to the west of this valley. Low positive values were also detected in the northern part of the agricultural Hama-Dori plain, facing the ocean, and in northwestern areas of the Abukuma plateau (e.g., Iitate and Katsurao towns). Significant negative values, down to −2, were expectedly observed in densely inhabited areas: Fukushima, Koriyama, and some coastal cities. This corroborates the assumption that urban radioactivity might have rapidly decreased from April to November 2011, through processes other than physical decay. Some negative values were also detected in the western volcano regions (e.g., west Koriyama, Inawishiro), but confidence in the kriged A_B field was rather low there (see section 2 of the SI). As shown in Figure 3b, large

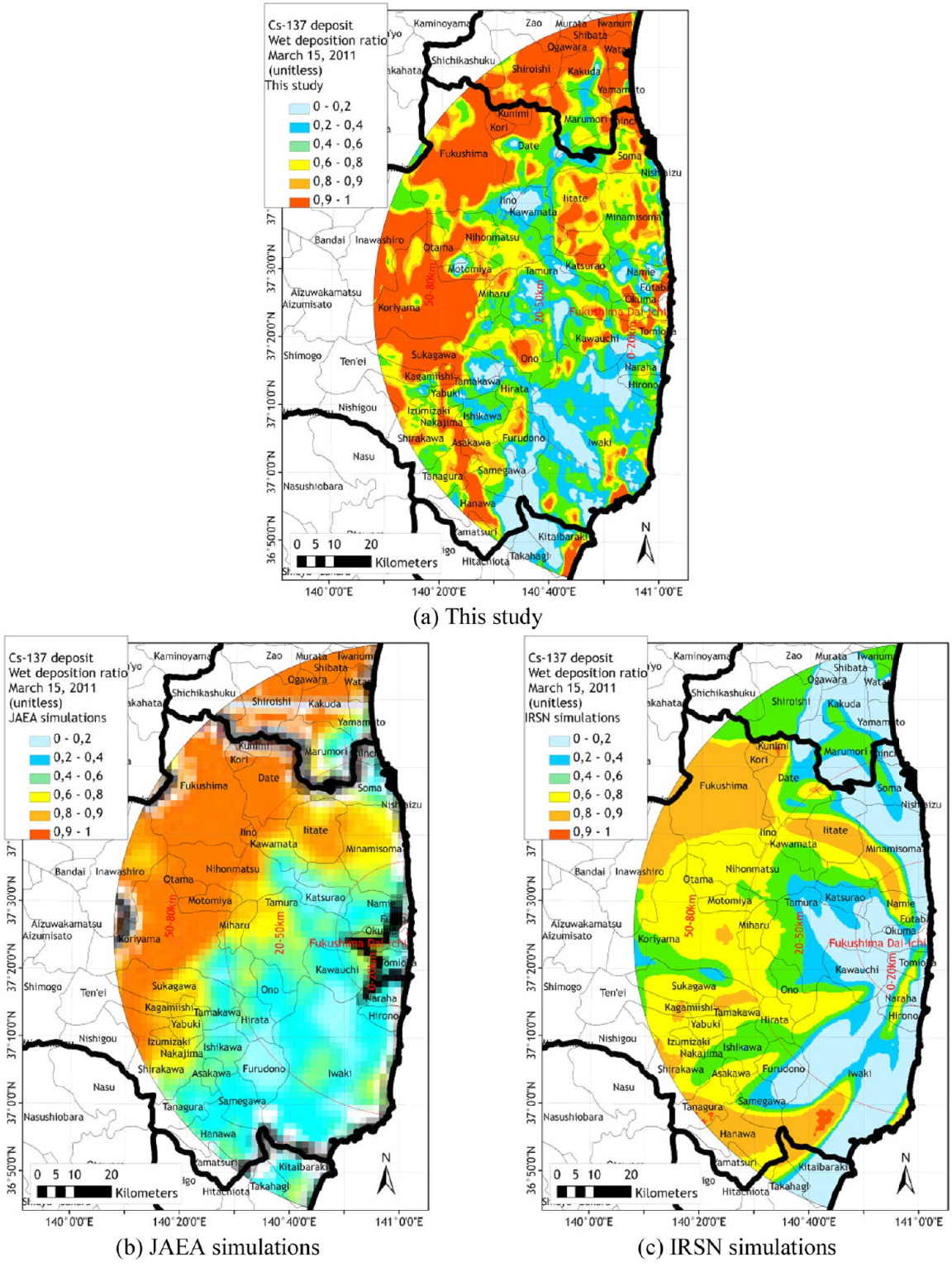

Figure 4. Computed spatial distribution of the wet fraction of ^{137}Cs deposits at the end of March 2011: (a) this study with a 300 m averaging radius and (VdW*, VdA*, VdU*, VdF*) = (0, 2, 2, 5), (b) by JAEA,[6] (c) by IRSN.[9] The map displayed in (b) has been produced by scanning the original picture, zooming in, georeferencing, legending and customizing under GIS software.

spatial spots of high positive values ($\beta > 0.6$, or $A_\Sigma > 3A_B$) were situated to the south−southwest of FDNPP, in high-elevation forested zones of the Abukuma mountains.

Spatial Distribution of Wet Deposition Ratio. The spatial estimation of wet atmospheric deposition ratio, 1-DR, is displayed in Figure 4a for a 300 m averaging radius and the lowest deposition velocity ratios. Sensitivity to the radius was shown to be limited here again. Adopting a 150 m radius increased the spatial variability in the small scale range but did not impact spatial predictions at scales greater than a kilometer. Sensitivity to the deposition velocity ratios was more important as deposits depend directly on $Vd_\Sigma^*/(Vd_\Sigma^*-1)$. The two

dx.doi.org/10.1021/es502590s | Environ. Sci. Technol. 2014, 48, 11268−11276

estimations differed by about 20% on the average. This calculated map confirms that intense wet deposition might have occurred in the Abukuma valley, as well as to the northwest of the nuclear site, in Namie, Katsurao and Iitate areas. On the contrary, a noticeable part of contamination might have been produced by dry deposition in the southwestern regions, most of these areas coinciding with high forested lands of the Abukuma range, where evergreen species are predominant. This spatial correlation suggests that dry deposition might have been enhanced in evergreen forest areas, at relatively high altitudes. This result is consistent with the observations/simulations by Katata et al. (2012) in which precipitation was shown to be relatively small around the mountain ridges above 500 m.

Comparison with Numerical Simulations. Atmospheric simulations can be used to better understand the processes that led to land contamination (releases and meteorological events) and to infer information that cannot be reconstructed through measurements alone (e.g., for dates or locations where no measurements were available, or for dose estimation). At a local scale, atmospheric simulations were conducted by JAEA[1,4−6] and IRSN.[8,9,7] The wet fraction of radiocaesium deposit inferred from these simulations (Figure 4b,c) can be compared to present result (Figure 4a).

JAEA's simulations were based on the WSPEEDI-II system,[26] using MM5 simulations forced with wind and rain observations for meteorological fields, and a Lagrangian particle model, GEARN, for dispersion. The source term was estimated through a reverse method using environmental measurements coupled with dispersion simulations, and included a few isotopes. The dry deposition velocity for cesium was set to 0.1 cm s^{-1} respectively, and five times larger for forest areas. The wet scavenging coefficient was given by eq 10 (see section 3 of the SI) with a unit rainfall scavenging rate $\Lambda^* = 5.10^{-5}$ s^{-1} and a scavenging power coefficient $\alpha = 0.8$.

IRSN's simulations were made with the Gaussian puff model pX, which is part of IRSN's operational modeling platform C3X. Meteorological forecasts from the European Center for Medium-Range Weather Forecasts (ECMWF) were used, with a resolution of 0.125° and a time step of 3 h. Observations were preferred over forecasts during the evening of March 15, with a time frequency of 10 min and a homogeneous wind field. Rain radar observations were used for the whole simulation period, with a 1 h time step. The source term included 73 radioisotopes, and the release kinetics was inferred from on-site information (pressure decreases, explosions. . .) completed with environmental data and simulations. The dry deposition velocity for particulate matter was set to 0.2 cm s^{-1}, whatever the landscape category is. The wet scavenging coefficient was given by eq 10 with $\Lambda^* = 5.10^{-5}$ s^{-1} and $\alpha = 1$.

Both numerical studies showed that two main rain events might have been responsible for local-scale predominantly wet deposition. The most important one occurred on March 15 during the early evening and the night, and the second occurred on 20−22 March. During the first episode, the wind was blowing from east, then southeast, before returning north on March 16. This event was mainly responsible for the high deposits to the northwest of FDNPP (see Figure 2) and further to the west in Abukuma valley. This episode was quite difficult to accurately reproduce on the basis of dispersion models, however, since all models failed to accurately forecast the changing wind direction during the few hours when the plume encountered precipitation coming from the northwest. These uncertainties in meteorology dynamics, due to complex orography, may explain discrepancies that are observed between numerical results and present estimation in the northwestern area. According to JAEA's simulations and present study estimations (Figure 4a,b), wet deposition might have also occurred on March 20, in the northern part of the 80 km region. IRSN's estimation failed to reproduce that event, due the absence of release at that time. All studies showed that dry deposition might have been predominant to the south−southwest of FDNPP. JAEA's and present studies agreed particularly well there, and predicted mostly dry deposition in Abukuma high lands occupied by evergreen coniferous species, predominantly. This findings are consistent with the increase of dry deposition velocity in dense forest areas.

This comparison shows that simulation results are quite consistent with the deposition ratio map derived from this study, at large scales. Small-scale structures are, however, much less satisfactorily captured by the models, mainly because of the spatiotemporal resolution of meteorological fields which failed to account for the complex orography and high-frequency wind fluctuations. Studies also suffered from the lack of information on cesium particle size distribution which prevented them from adopting refined microphysical parametrizations for deposition and scavenging of atmospheric aerosols. Furthermore, all source term reconstructions so far are (partially or totally) based on environmental measurements and dispersion simulations, which make them dependent on simulation and measurement uncertainties.[1,27,8,28,29] Therefore, model-to-observation discrepancies are bound to exist, especially at small spatial scales, and the agreement observed on Figure 4a,b,c can be deemed reasonable.

Significance of Methodology. The methodology developed in this paper to estimate dry and wet deposited fractions of gamma-emitting radionuclides proved to give reasonable results for cesium deposits in the Fukushima region. The results are noteworthy in that (i) distribution of the dry/wet deposition ratio reasonably agrees with physically based atmospheric predictions at large spatial scales, (ii) positive anomalies in land surface deposit have been detected in evergreen forest regions where, as expected, dry deposition might have been enhanced, and (iii) negative anomalies have been detected in large urban areas where, as expected, rapid decontamination through natural wash-off and anthropogenic processes has likely occurred. These results proved to be rather insensitive to modeling assumptions and parameter choices. Confidence in the predicted maps is especially high in forested areas where, precisely, it is important to properly predict the interception fraction by canopies. Results, however, remain sensitive to the imprecision in field observations, in regions were bare soil and land surface deposits do not much differ (no or weak anomalies). Unfortunately, uncertainty analysis could not be performed in the present study because errors associated with deterministic airborne measurements were not available. Finally, an important point is that the sum of dry and wet deposits predicted at all locations by our method (see eq 6) does exactly match the total deposit measured by airborne survey (unlike atmospheric simulations which produce deposition maps that are not fully consistent with field observations).

As such, this methodology has the possibility to contribute information that can be applied to the understanding of the impacts of this specific nuclear accident, in the course of ongoing and future assessment studies of doses to humans and

the environment. The importance of accounting for spatial variability in dry and wet deposition, as we have shown herein, is also pertinent to many nonradioactive pollutants that disperse by atmospheric processes and deposit via dry and wet processes.

In case of a nuclear accident, this methodology might stand as a complementary approach to more sophisticated numerical studies. As it relies on gamma-ray spectrometry data which will likely be produced in the very first days or weeks after an accident, the method could be invoked quite early in the assessment cycle. Another advantage is that the analysis would be easy to carry out and would require little additional knowledge—a high-resolution landuse map and an estimate of the physical form of deposited materials.

■ ASSOCIATED CONTENT

Supporting Information

Supporting Information includes five sections dealing with geostatistical and deposition modeling assumptions. This material is available free of charge via the Internet at http://pubs.acs.org

■ AUTHOR INFORMATION

Corresponding Author

*Phone +33-442-199-544; fax +33-442-199-608; e-mail: marc-andre.gonze@irsn.fr.

Notes

The authors declare no competing financial interest.

■ REFERENCES

(1) Chino, M.; Nakayama, H.; Nagai, H.; Terada, H.; Katata, G.; Yamazawa, H. Preliminary estimation of release amounts of ^{131}I and ^{137}Cs accidentally discharged from the Fukushima Daiichi nuclear power plant into atmosphere. *J. Nucl. Sci. Technol.* **2011**, *48*, 1129–1134.

(2) Morino, Y.;Ohara, T.;Nishizawa, M. Atmospheric behavior, deposition and budget ofradioactive materials from the Fukushima Daiichi nuclear power plant in March 2011. *Geophys. Res. Lett.* **2011**, *38*(7), L00G11, 1–28, DOI: 10.1029/2011GL048689.

(3) Yasunari, T. J.; Stohl, A.; Hayano, R. S.; Burkhart, J. F.; Eckhardt, S.; Yasunari, T. Cesium-137 deposition and contamination of Japanese soils due to the Fukushima nuclear accident. *Proc. Natl. Acad. Sci. U.S.A.* **2011**, *108* (49), 19530–19534, DOI: 10.1073/pnas.1112058108.

(4) Katata, G.; Ota, M.; Terada, H.; Chino, M.; Nagai, H. Atmospheric discharge and dispersion of radionuclides during the Fukushima Daiichi Nuclear Power Plant accident. Part I: Source term estimation and local-scale atmospheric dispersion in early phase of the accident. *J. Environ. Radioact.* **2012**, *109*, 103–113, DOI: 10.1016/j.jenvrad.2012.02.006.

(5) Katata, G.; Ota, M.; Terada, H.; Chino, M.; Nagai, H. Atmospheric discharge and dispersion of radionuclides during the Fukushima Daiichi Nuclear Power Plant accident. Part I: Source term estimation and local-scale atmospheric dispersion in early phase of the accident. *J. Environ. Radioact.* **2012**, *109*, 103–113, DOI: 10.1016/j.jenvrad.2012.02.006.

(6) Terada, H.; Katata, G.; Chino, M.; Nagai, H. Atmospheric discharge and dispersion of radionuclides during the Fukushima Daiichi Nuclear Power Plant accident. Part II: verification of the source term and analysis of regional-scale atmospheric dispersion. *J. Environ. Radioact.* **2012**, *112*, 141–154, DOI: 10.1016/j.jenvrad.2012.05.023.

(7) Champion, D.; Korsakissok, I.; Didier, D.; Mathieu, A.; Quélo, D.; Groel, J.; Quentric, E.; Tombette, M.; Benoit, J.-P.; Saunier, O.; Parache, V.; Simon-Cornu, M.; Gonze, M.-A.; Renaud, P.; Cessac, B.; Navarro, E.; Servant-Perrier, A.-C. The IRSN's earliest assessments of the Fukushima accident's consequences for the terrestrial environment in Japan. *Radioprotection* **2013**, *48* (1), 11–37, DOI: 10.1051/radiopro/2012052.

(8) Mathieu, A.; Korsakissok, I.; Quélo, D.; Groel, J.; Tombette, M.; Didier, D.; Quentric, E.; Saunier, O.; Benoit, J.-P.; Isnard, O. Atmospheric dispersion and deposition of radionuclides from theFukushima Daiichi nuclear power plant accident. *Elements* **2012**, *8* (3), 195–200, DOI: 10.2113/gselements.8.3.195.

(9) Korsakissok, I.; Mathieu, A.; Didier, D. Atmospheric dispersion and ground deposition induced by the Fukushima Nuclear power plant accident: A local-scale simulation and sensitivity study. *Atmos. Environ.* **2013**, *70*, 267–279, DOI: 10.1016/j.atmosenv.2013.01.002.

(10) Morino, Y.; Ohara, T.; Watanabe, M.; Hayashi, S.; Nishizawa, M. Episode analysis of deposition of radiocesium from the Fukushima Daiichi Nuclear Power Plant Accident. *Environ. Sci. Technol.* **2013**, *47* (5), 2314–2322, DOI: 10.1021/es304620x.

(11) Zhang, L.; Gong, S.; Padro, J.; Barrie, L. A size-segregated particle dry deposition scheme for an atmospheric aerosol module. *Atmos. Environ.* **2001**, *35* (3), 549–560, DOI: 10.1016/S1352-2310(00)00326-5.

(12) Petroff, A.; Mailliat, A.; Amielh, M.; Anselmet, F. Aerosol dry deposition on vegetation canopies. Part I: Review of present knowledge. *Atmos. Environ.* **2008**, *42*, 3625–3653.

(13) Petroff, A.; Mailliat, A.; Amielh, M.; Anselmet, F. Aerosol dry deposition on vegetation canopies. Part II: A new modelling approach and applications. *Atmos. Environ.* **2008**, *42*, 3654–3683.

(14) *Quantification of Radionuclide Transfer in Terrestrial and Freshwater Environments for Radiological Assessments*, IAEA-TEC-DOC-1616; International Atomic Energy Agency, 2009; pp616.

(15) Pröhl, G. Interception of dry and wet deposited radionuclides by vegetation. *J. Environ. Radioact.* **2009**, *100* (9), 675–682, DOI: 10.1016/j.jenvrad.2008.10.006.

(16) Petroff, A.; Zhang, L.; Pryor, S. C.; Belot, Y. An extended dry deposition model for aerosols onto broadleaf canopies. *Aerosol Sci.* **2009**, *40*, 218–240, DOI: 10.1016/j.jaerosci.2008.11.006.

(17) Petroff, A.; Zhang, L. Development and validation of a size-resolved particle dry deposition scheme for application in aerosol transport models. *Geosci. Model Dev.* **2010**, *3*, 753–769, DOI: 10.5194/gmd-3-753-2010.

(18) Hoffman, F. O.; Thiessen, K. M.; Frank, M. L.; Blaylock, B. G. Quantification of the interception and initial retention of radioactive contaminants deposited on pasture grass by simulated rain. *Atmos. Environ.* **1992**, *26* (18), 3313–3321, DOI: 10.1016/0960-1686(92)90348-O.

(19) Müller, H.; Pröhl, G. ECOSYS-87: A dynamic model for assessing radiologicalconsequences of nuclear accidents. *Health Phys.* **1993**, *64* (3), 232–252.

(20) Hoffman, F. O.; Thiessen, K. M.; Rael, R. M. Comparison of interception and initial retention of wet-deposited contaminants on leaves of different vegetation types. *Atmos. Environ.* **1995**, *29* (15), 1771–1775.

(21) *Modelling of radionuclide interception and loss processes in vegetation and of transfer in semi-natural ecosystems. Second report of the VAMP Terrestrial Working Group*, IAEA-TECDOC-857; International Atomic Energy Agency, 1996; pp84.

(22) Kinnersley, R. P.; Goddard, A. J. H.; Minski, M. J.; Shaw, G. Interception of caesium contaminated rain by vegetation. *Atmos. Environ.* **1997**, *31* (8), 1137–145, DOI: 10.1016/S1352-2310(96)00312-3.

(23) *Results of the Research on Distribution of Radioactive Substances Discharged by the Accident at TEPCO's Fukushima Daiichi NPP*; Japanese Nuclear Regulatory Authority Website. http://radioactivity.nsr.go.jp/en/list/269/list-1.html (accessed on March 27, 2014).

(24) *Summarized Version of the "Results of the Research on Distribution of Radioactive Substances Discharged by the Accident at TEPCO's Fukushima Dai-ichi NPP*; Emergency Operation Center, Ministry of Education, Culture, Sports, Science and Technology Agriculture, Forestry and Fisheries Research Council, Ministry of Agriculture, Forestry and Fisheries. http://radioactivity.nsr.go.jp/en/contents/1000/294/24/PressR04%200802s.pdf (accessed on March 27, 2014).

(25) *Airborne Monitoring Survey Results*; Japanese Nuclear Regulatory Authority Website. http://radioactivity.nsr.go.jp/en/list/270/list-1.html (accessed on March 27, 2014).
(26) Terada, H.; Nagai, H.; Furuno, A.; Kakefuda, T.; Harayama, T.; Chino, M. Development of worldwide version of system for prediction of environmental emergency dose information: WSPEEDI 2nd version. *Trans. At. Energy Soc. Jpn.* **2008**, *7* (3), 257−267 in Japanese with English abstract.
(27) Stohl, A.; Seibert, P.; Wotawa, G.; Arnold, D.; Burkhart, J. F.; Eckhardt, S.; Tapia, C.; Vargas, A.; Yasunari, T. J. Xenon-133 and caesium-137 releases into the atmosphere from the Fukushima Daiichi nuclear power plant: determination of the source term, atmospheric dispersion, and deposition. *Atmos. Chem. Phys. Discuss.* **2011**, *11*, 28319−28394, DOI: 10.5194/acpd-11-28319-2011.
(28) Saunier, O.; Mathieu, A.; Didier, D.; Tombette, M.; Quélo, D.; Winiarek, V.; Bocquet, M.; Saunier, O.; Mathieu, A.; Didier, D.; Tombette, M.; Quélo, D.; Winiarek, V.; et Bocquet, M. An inverse modeling method to assess the source term of the Fukushima Nuclear Power Plant accident using gamma dose rate observations. *Atmos. Chem. Phys.* **2013**, *13* (22), 11403−11421 2013.
(29) Winiarek, V.; Bocquet, M.; Saunier, O.; Mathieu, A. Estimation of errors in the inverse modeling of accidental release of atmospheric pollutant: application to the reconstruction of the cesium-137 and iodine-131 source terms from the Fukushima Daiichi power plant. *J. Geophys. Res.* **2012**, *117*, D05122 DOI: 10.1029/2011JD016932.